

Many-body theory of core holes

L. S. Cederbaum

Lehrstuhl für Theoretische Chemie, Institut für Physikalische Chemie, Universität Heidelberg, 69 Heidelberg, Germany

W. Domcke and J. Schirmer

Fakultät für Physik, Universität Freiburg, 78 Freiburg, Germany

(Received 15 October 1979)

An electronic Hamiltonian appropriate for describing core-hole processes is derived and its properties are discussed. Based on this Hamiltonian a many-body theory is presented, and a useful linked-cluster theorem is proven. A distinction between relaxation and correlation terms can be made in each order of the perturbation expansion. Under certain well-defined conditions the core-ionization process can be visualized as a Franck-Condon transition between two multidimensional potential-energy surfaces in an abstract bosonic space. The corresponding approximation, the boson approximation, is discussed and applied to the water molecule.

I. INTRODUCTION

The study of core-hole properties has been popular over the last years. Improved experimental techniques¹ have stimulated intense theoretical interest in the subject. Theoretical work on core-hole properties has been done for atoms and molecules,^{2,3} solids,⁴ and chemisorbed systems.⁵ In the latter two cases one usually starts the calculation by introducing a model Hamiltonian which accounts for the effects to be explained. For atoms and molecules there exist computational methods which make accessible a more quantitative agreement with experiment. Most of the molecular core-hole properties of interest can, in principle, be calculated by performing separate Hartree-Fock computations, one on the initial state and one on the final state involved in the process under consideration, supplemented by one or another configuration interaction method. Nearly all theoretical studies on atoms and molecules make use of this or a closely related procedure. Although such procedures may lead to satisfactory results, they treat the initial and final states differently and are often strongly numerically oriented.

In the present contribution we attempt to derive an electronic Hamiltonian suitable for describing core-hole processes by starting from the full Hamiltonian and making use of properties inherent to core levels. The same Hamiltonian applies for both the initial and the final states. In addition, we hope that such a Hamiltonian can be used to identify the different types of effects involved in a given core-hole process. In this way model Hamiltonians can be constructed which aim at the direct explanation of the dominating effects as done, for example, to explain the multipole structure in core-hole spectra of highly polar disubstituted aromatic systems.⁶

In the second part of the manuscript a many-body theory to evaluate the core-hole spectrum is presented. We shall see that the introduction of the "core Hamiltonian" enables us to derive relations which simplify the many-body approach and make it more transparent for interpretation purposes. At the moment we do not aim at obtaining highly accurate numbers; our goal is rather to gain insight into core-hole processes which is complementary to that obtained by the commonly used computational approaches.

II. THE HAMILTONIAN

To arrive at a Hamiltonian which is appropriate for describing both the electronic system and its ion, we adopt the formalism of second quantization. Defining annihilation and creation operators a_k and a_k^\dagger for an electron in a one-particle state $|\varphi_k\rangle$, the electronic Hamiltonian reads

$$H = \sum_i \epsilon_i a_i^\dagger a_i + \sum_{i,j} v_{ij} a_i^\dagger a_j + \frac{1}{2} \sum_{i,j,k,l} V_{ijkl} a_i^\dagger a_j^\dagger a_l a_k, \quad (1)$$

where ϵ_i , v_{ij} , and V_{ijkl} are the matrix elements of an unperturbed Hamiltonian H_0 , a one-particle potential v , and of the Coulomb interaction between the electrons:

$$V_{ijkl} = \langle \varphi_i(r) \varphi_j(r') | |r - r'|^{-1} | \varphi_k(r) \varphi_l(r') \rangle,$$

respectively. $\{\varphi_i\}$ is any orthogonal basis of spin orbitals that diagonalizes H_0 . The potential v can, in principle, include an external potential.

Without loss of generality we choose H_0 to be the Hartree-Fock (HF) operator. Then the ϵ_i become the HF orbital energies and, if no external potential is included, we have

$$v_{ij} = - \sum_k (V_{ikjk} - V_{ikhj}) n_k, \quad (2)$$

where n_k is the occupation number of the orbital φ_k in the HF ground state; i.e., $n_k=1$ if φ_k is occupied in the HF ground state and $n_k=0$ otherwise. In case the so-called spin-unrestricted HF operator⁷ is chosen, Eq. (2) is valid for both closed-shell and open-shell systems. On the other hand, if we choose H_0 to be the so-called spin-restricted HF operator,⁸ we have to distinguish between the closed-shell and the open-shell cases. Whereas Eq. (2) is still correct for closed-shell systems, the choice of v_{ij} is somewhat ambiguous for open-shell systems and depends on the special method chosen.⁸ For the sake of simplicity we restrict ourselves in the following to closed-shell systems, but would like to point out that the theory below can straightforwardly be rewritten to apply to open-shell systems as well.

In the following we attempt to simplify the Hamiltonian (1) by making explicit use of the genuine properties of (deep) core orbitals. We assume for the moment that each core orbital is strongly localized on its corresponding atomic site. Consequently, a hole in the core orbital φ_{c_1} has a very low probability of propagating to core orbital φ_{c_2} even if the core-hole energies are similar and the Hamiltonian used to determine the ionization spectrum of a specific core orbital φ_c need not contain the remaining core orbitals. We may, therefore, proceed by taking into account only a single core hole. Because of the large difference in energy and in the localization in space between core and valence orbitals, it is commonly accepted that the solutions of the Schrödinger equation can be separated to a good approximation into a core and a valence part.⁹ This separability between core and valence electrons can be achieved by omitting all terms of H in (1) which include a different number of core creation operators a_c^\dagger and core annihilation operators a_c . After some straightforward algebra the resulting Hamiltonian H_{cv} reads

$$H_{cv} = H_v + H_c + W_{cv} + F_{cv}. \quad (3)$$

The operator H_v denotes the Hamiltonian of the valence electrons, i.e.,

$$H_v = \sum_i \epsilon_i a_i^\dagger a_i - \sum_{ij} \left(\sum_k (V_{ikjk} - V_{ikhj}) n_k \right) a_i^\dagger a_j + \frac{1}{2} \sum_{i,j,k,l} V_{ijkl} a_i^\dagger a_j^\dagger a_l a_k, \quad (4a)$$

where here and in the following the indices i, j, k , and l do not include the core index c . H_c is the Hamiltonian of the core electrons and is given by

$$H_c = \epsilon_c (\hat{n}_{c\uparrow} + \hat{n}_{c\downarrow}) + V_{ccc} \hat{n}_{c\uparrow} \hat{n}_{c\downarrow} + (\hat{n}_{c\uparrow} + \hat{n}_{c\downarrow}) v_{cc}, \quad (4b)$$

where we have introduced the occupation-number operator $\hat{n}_m = a_m^\dagger a_m$ (not to be confused with the HF ground-state occupation number n_m) and denote the one-electron spin indices by \uparrow and \downarrow . The interaction term

$$F_{cv} = \left(- \sum_{ij} V_{ic\uparrow c\downarrow j} a_i^\dagger a_j \right) a_{c\uparrow}^\dagger a_{c\downarrow} + \text{c.c.} \quad (4c)$$

does not preserve the spin of the core electrons, and we refer to it as the spin-flip term. The second interaction term reads

$$W_{cv} = - (1 - \hat{n}_{c\uparrow}) \sum_{ij} (V_{ic\uparrow j c\uparrow} - V_{ic\uparrow c\downarrow j}) a_i^\dagger a_j + (c\uparrow \rightarrow c\downarrow). \quad (4d)$$

The Hamiltonian (3) has several interesting properties which should be discussed. The separability of core and valence electrons implies that the number of core electrons is an invariant quantity. Introducing the core-electron number operator

$$\hat{N}_c = \hat{n}_{c\uparrow} + \hat{n}_{c\downarrow},$$

it can easily be shown that it commutes with H_{cv}

$$[\hat{N}_c, H_{cv}] = 0. \quad (5)$$

Clearly $\hat{N}_v = \sum_i \hat{n}_i$ also commutes with H_{cv} , since the electron number operator $\hat{N} = \hat{N}_c + \hat{N}_v$ commutes with H_{cv} . The spin-flip term F_{cv} can be neglected in many types of calculations, because its matrix elements V_{iccj} are exchange Coulomb integrals between core and valence orbitals and thus small. Nevertheless, F_{cv} must be included in H_{cv} in order to guarantee the correct spin symmetry. The first of the relations

$$[\hat{S}^2, H_{cv}] = 0, [\hat{S}_z, H_{cv}] = 0 \quad (6)$$

only holds if F_{cv} is included in H_{cv} .

When F_{cv} is neglected, both $\hat{n}_{c\uparrow}$ and $\hat{n}_{c\downarrow}$ commute with H_{cv} , and a straightforward interpretation of the relevant interaction term is possible. In the ground state both core spin orbitals are occupied, and $\hat{n}_{c\uparrow}$, $\hat{n}_{c\downarrow}$ can be replaced by 1. Consequently, $W_{cv} = 0$ in the ground state, and the valence-core parts do not interact.¹⁰ When a core hole of spin \uparrow is created, the final Hamiltonian is obtained by putting $\hat{n}_{c\uparrow} = 1$ and $\hat{n}_{c\downarrow} = 0$. The valence orbitals now "feel" a one-particle potential

$$W_{cv} = - \sum_{ij} (V_{ic\uparrow j c\uparrow} - V_{ic\uparrow c\downarrow j}) a_i^\dagger a_j$$

and relax. By redefining the valence-orbital basis, one can eliminate this term and obtain $H_{cv} = H_v + H_c$, again finding no interaction between the core and valence parts. H_v is still given by Eq. (4a), but all quantities and operators appearing there should be replaced by the "relaxed" ones, i.e., H_v is the valence Hamiltonian written in the basis of orbit-

als determined from a self-consistent HF calculation on the system with a core hole.

The Hamiltonian (3) does not describe the broadening of core-hole levels due to the emission of Auger electrons. For core holes in light atoms this broadening is small and is negligible compared to the vibrational broadening in molecules¹¹ and probably also in solids.¹² The vibrational structure in core-hole spectra of molecules can be calculated using (3) and taking into account that the ϵ_m and V_{mnsr} are functions of the internuclear distances.¹³ In principle, the Auger broadening can also be calculated via (3) if an "Auger term" is added to H_{cv} .

The Hamiltonian (3) has been derived assuming the core orbitals to be localized each on another atomic site. The derivation of an adequate Hamiltonian becomes more complex when core orbitals are delocalized over several equivalent atomic sites due to symmetry requirements. In this case

a core hole has a high probability of propagating to its quasidegenerate counterparts, since they are all confined to the same space. We consider in the following two core orbitals φ_{c_g} and φ_{c_u} which are delocalized over the two equivalent atomic sites s_1 and s_2 . Applying the same rules as used to derive H_{cv} in (3), i.e., the number of core creation operators must be equal in every term of the Hamiltonian to the number of core annihilation operators, we obtain

$$H_{cv} = H_v + H_{c_g}^v + H_{c_u}^v + W_{c_g c_u} + W_{c_g c_u}^v. \quad (7)$$

Here H_v is the same valence Hamiltonian as in (3) and $H_{c_g}^v$, $H_{c_u}^v$ are given by the sum $H_c + W_{cv} + F_{cv}$ in (3) for $c = c_g$ and $c = c_u$, respectively. The Hamiltonians $H_{c_g^v} \equiv H_v + H_{c_g}^v$ and $H_{c_u^v} \equiv H_v + H_{c_u}^v$ thus describe the electronic system with only one active core orbital φ_{c_g} or φ_{c_u} . The direct interaction between the core states is described by the term

$$W_{c_g c_u} = V_{c_g c_u c_g c_u} (\hat{n}_{c_g \uparrow} \hat{n}_{c_u \downarrow} + \hat{n}_{c_g \downarrow} \hat{n}_{c_u \uparrow}) + (V_{c_g c_u c_g c_u} - V_{c_g c_u c_u c_g}) (\hat{n}_{c_g \uparrow} \hat{n}_{c_u \uparrow} + \hat{n}_{c_g \downarrow} \hat{n}_{c_u \downarrow}) + V_{c_g c_g c_u c_u} (a_{c_g \uparrow}^\dagger a_{c_u \uparrow} + a_{c_u \uparrow}^\dagger a_{c_g \uparrow}) (a_{c_g \downarrow}^\dagger a_{c_u \downarrow} + a_{c_u \downarrow}^\dagger a_{c_g \downarrow}), \quad (8a)$$

while the remaining interaction term reads

$$W_{c_g c_u}^v = \left(a_{c_g \uparrow}^\dagger a_{c_u \uparrow} \sum_{i,j} (V_{i c_g \uparrow j c_u \uparrow} - V_{i c_g \uparrow c_u \uparrow j}) a_i^\dagger a_j + (c \uparrow \leftrightarrow c \downarrow) \right) - \left(a_{c_g \uparrow}^\dagger a_{c_u \downarrow} \sum_{i,j} V_{i c_g \uparrow c_u \downarrow j} a_i^\dagger a_j + (c \uparrow \leftrightarrow c \downarrow) \right) + \text{c.c.} \quad (8b)$$

To arrive at a better understanding of (7) we consider the core orbitals φ_{c_g} and φ_{c_u} as linear combinations of nonsymmetry-adapted orbitals φ_{s_1} and φ_{s_2} which are strongly localized ($\varphi_{s_1} \varphi_{s_2} = 0$) on the atomic sites s_1 and s_2 :

$$\begin{aligned} \varphi_{c_g} &= (1/\sqrt{2})(\varphi_{s_1} + \varphi_{s_2}), \\ \varphi_{c_u} &= (1/\sqrt{2})(\varphi_{s_1} - \varphi_{s_2}). \end{aligned} \quad (9)$$

Using this simple relation we can easily rewrite the Hamiltonian (7) and obtain the more transparent result

$$H_{cv} = H_v + H_{s_1}^v + H_{s_2}^v + W_{s_1 s_2} + W_{s_1 s_2}^v. \quad (10)$$

The operators $H_{s_1}^v \equiv H_v + H_{s_1}^v$ and $H_{s_2}^v \equiv H_v + H_{s_2}^v$ are the Hamiltonians of the system with one active localized core orbital and are each equal to H_{cv} in (3) with $c = s_1$ and s_2 , respectively. The term describing the direct interaction between the localized core orbitals simplifies considerably to the following expression

$$W_{s_1 s_2} = V_{s_1 s_2 s_1 s_2} \hat{N}_{s_1} \hat{N}_{s_2}, \quad (11a)$$

where $\hat{N}_{s_i} = \hat{n}_{s_i \uparrow} + \hat{n}_{s_i \downarrow}$ is the core-electron occupation operator at the atomic site s_i . The remaining interaction term in (10) is given by

$$\begin{aligned} W_{s_1 s_2}^v &= - \left(a_{s_1 \uparrow}^\dagger a_{s_2 \uparrow} \sum_{i,j} V_{i s_1 \uparrow s_2 \uparrow j} a_i^\dagger a_j + (s \uparrow \leftrightarrow s \downarrow) \right) \\ &\quad - \left(a_{s_1 \uparrow}^\dagger a_{s_2 \downarrow} \sum_{i,j} V_{i s_1 \uparrow s_2 \downarrow j} a_i^\dagger a_j \right. \\ &\quad \left. + (s \uparrow \leftrightarrow s \downarrow) \right) + \text{c.c.} \end{aligned} \quad (11b)$$

Interestingly the interaction term $W_{s_1 s_2}^v$ contains only exchange matrix elements involving two core orbitals strongly localized on different atomic sites and represents, therefore, a weak interaction. The interaction term $W_{c_g c_u}^v$, on the other hand, gives rise to a strong interaction between the delocalized core orbitals via the valence orbitals. When $W_{s_1 s_2}^v$ is neglected, each of the core occupation operators $\hat{n}_{s_1 \uparrow}$, $\hat{n}_{s_1 \downarrow}$, $\hat{n}_{s_2 \uparrow}$, and $\hat{n}_{s_2 \downarrow}$ commutes with the Hamiltonian (10). Hence, these operators can be replaced by the occupation num-

bers according to the core occupancy in a given state. In the ground state all \hat{n}_{s_i} can be replaced by 1 and one finds that there is no core-valence interaction. If an electron is ejected off the orbital φ_{s_1} , the operators $\hat{n}_{s_2\uparrow}$ and $\hat{n}_{s_2\downarrow}$ are still equal to 1 and the resulting final state Hamiltonian does not include any interaction between φ_{s_2} and the valence orbitals or the core orbital φ_{s_1} [the trivial term $W_{s_1s_2}$ (ground state) - $W_{s_1s_2}$ (core-hole state) = $V_{s_1s_2s_1s_2}$ is compensated by integrals of $v_{s_1s_2}$ in H_{s_1}].

We have thus shown that abandoning the symmetry restriction on the orbital basis allows a separate treatment of each of the core-hole spectra via H_{cv} in (3) which is the Hamiltonian of a system with a single active core orbital. The strong correlation term $W_{c_p c_u}^v$ present when operating with the symmetry-adapted basis is incorporated into a relaxation term in the symmetry-nonadapted basis.¹⁴ This explains the good results obtained with Δ SCF calculations using localized orbitals, first demonstrated by Bagus and Schaefer.¹⁵

Finally we would like to mention that the Hamiltonian (7) describes several additional interesting features in the more complicated case where the core orbitals φ_{c_g} and φ_{c_u} are not strictly degenerate. Such cases are given, e.g., by molecules at short interatomic separations or when investigating intermediate core orbitals where φ_{s_1} and φ_{s_2} have a nonvanishing overlap. It is then convenient to perform a transformation similar to (9) and to consider the additional terms in H_{cv} which arise due to the nonvanishing overlap as a perturbation.

III. THE CORE-HOLE SPECTRUM

The Hamiltonian H_{cv} in (3) can be used to obtain a wealth of information on processes involving a change in the number of core electrons. The simplest process of this kind is the ionization of a core orbital. The rest of this paper is devoted to the calculation and interpretation of the resulting spectrum, which is usually referred to as the core-hole spectrum.

Using the sudden approximation,¹⁶⁻¹⁸ the core-hole spectrum $P(\omega)$ as a function of energy ω is given by

$$P(\omega) \approx \text{Im} G_{c\uparrow c\uparrow}(\omega) + \text{Im} G_{c\uparrow c\downarrow}(\omega), \quad (12)$$

where $G_{mn}(\omega)$ is the Fourier transform of the one-body Green's function^{19, 20}

$$G_{mn}(t) = -i \langle \Psi_0^N | T [a_m(t) a_n^\dagger] | \Psi_0^N \rangle. \quad (13)$$

$|\Psi_0^N\rangle$ denotes the ground-state wave function of the system having N electrons and T is the Wick time-

ordering operator. It should be mentioned that since we consider a closed-shell system, $G_{c\uparrow c\uparrow}$ is equal to $G_{c\downarrow c\downarrow}$. We now define ionic Hamiltonians $H_{cv}(0, 1)$ and $H_{cv}(1, 0)$ which are determined from $H_v + H_c + W_{cv}$ in (3) by putting ($\hat{n}_{c\uparrow}=0, \hat{n}_{c\downarrow}=1$), and ($\hat{n}_{c\uparrow}=1, \hat{n}_{c\downarrow}=0$), respectively. Introducing furthermore the operator

$$\hat{X} = \sum_{i,j} V_{iccj} a_{i\uparrow}^\dagger a_{j\uparrow},$$

we find

$$\begin{aligned} H_{cv} a_{c\uparrow} | \Psi_0^N \rangle &= H_{cv}(0, 1) a_{c\uparrow} | \Psi_0^N \rangle + \hat{X} a_{c\uparrow} | \Psi_0^N \rangle, \\ H_{cv} a_{c\downarrow} | \Psi_0^N \rangle &= H_{cv}(1, 0) a_{c\downarrow} | \Psi_0^N \rangle + \hat{X}^\dagger a_{c\downarrow} | \Psi_0^N \rangle. \end{aligned} \quad (14)$$

With the aid of these relations, the core-hole spectrum (12) can be rewritten to give

$$P(\omega) \approx \int_{-\infty}^{\infty} dt \exp[i(\omega - E_0^{Nv})t] \langle \vec{0} | e^{i\mathcal{H}t} | \vec{0} \rangle, \quad (15)$$

where E_0^{Nv} denotes the valence part of the ground-state energy

$$\begin{aligned} (H_v | \Psi_0^{Nv} \rangle &= E_0^{Nv} | \Psi_0^{Nv} \rangle) \text{ and} \\ \mathcal{H} &= \begin{pmatrix} H(\uparrow) & \hat{X} \\ \hat{X}^\dagger & H(\downarrow) \end{pmatrix}, \quad | \vec{0} \rangle = \begin{pmatrix} | \Psi_0^{Nv} \rangle \\ | \Psi_0^{Nv} \rangle \end{pmatrix}. \end{aligned} \quad (16a)$$

\mathcal{H} is a matrix Hamiltonian of dimension N_c (number of core electrons) and is independent of core operators and

$$\begin{aligned} H(\alpha) &= -\epsilon_c + H_v - \sum_{i,j} (V_{ic\alpha jc\alpha} - V_{ic\alpha c\alpha j}) \\ &\quad \times (a_i^\dagger a_j - n_i \delta_{ij}), \quad \alpha = \uparrow, \downarrow. \end{aligned} \quad (16b)$$

Expression (15) for a core-hole spectrum contains only valence operators. The only explicit dependence on core properties is via the HF orbital energy ϵ_c and the Coulomb integrals V_{icjc} and V_{iccj} . In principle, one can evaluate the spectrum via (15) by performing a configuration-interaction calculation for the matrix Hamiltonian \mathcal{H} similarly to the case of vibronic interaction in molecules.²¹ To this end one can use the eigenfunctions Ψ_m^{Nv} of H_v to construct a supermatrix A with 2×2 matrices $\langle \Psi_m^{Nv} | \mathcal{H} | \Psi_n^{Nv} \rangle$ as elements. Since \hat{X} is a spin-nonconserving operator, the supermatrix A decouples into two submatrices A_1 and A_2 which are essentially identical. The eigenvalues of A_1 give the positions of the lines in the spectrum and the square of the first element of the corresponding eigenvectors yields the (relative) intensities of these lines. This and related methods are numerically elaborate because of the large matrices which have to be diagonalized. Furthermore, many eigenvalues and eigenvectors of A_1 are of interest, but the efficient diagonalization methods for large matrices are

suitable for the calculation of only a few low-lying eigenstates. The situation simplifies considerably if \hat{X} is neglected in the calculation of $P(\omega)$. Then the core-hole spectrum becomes

$$P(\omega) \sim \int_{-\infty}^{\infty} dt \exp[i(\omega - E_0^{Nv})t] \times \langle \Psi_0^{Nv} | e^{iH(\alpha)t} | \Psi_0^{Nv} \rangle, \quad \alpha = \uparrow \text{ or } \downarrow. \quad (17)$$

It is shown in the following sections that this equation has several interesting properties which simplify its evaluation. Since \hat{X} is a weak-interaction term which originates from the spin-flip term F_{cv} in Eq. (4c), it can be neglected to a good approximation. The effect of \hat{X} on the spectrum can be determined separately by diagonalizing matrices A_1 of very low dimensions including only those nearly degenerate states of $H(\uparrow)$ and $H(\downarrow)$ in (16a) which are coupled via \hat{X} .

To estimate the effect of \hat{X} on the main line in the core-hole spectrum we give the expression for the ionization potential I_c in second-order perturbation theory as determined from Eq. (15):

$$I_c = -\epsilon_c - \sum_{j,i} \frac{2V_{jcl}^2 + 2V_{jcc}^2 - 2V_{jcl}V_{jcc}}{\epsilon_j - \epsilon_i} n_i(1 - n_j), \quad (18a)$$

where l denotes the valence orbitals doubly occupied in the HF ground state and j the empty orbitals. The corresponding expression derived from Eq. (17) reads

$$I_c = -\epsilon_c - \sum_{j,i} \frac{2V_{jcl}^2 + V_{jcc}^2 - 2V_{jcl}V_{jcc}}{\epsilon_j - \epsilon_i} n_i(1 - n_j). \quad (18b)$$

We have calculated the difference between (18a) and (18b) for the water molecule and obtained -0.12 eV, which is to be compared with $I_c + \epsilon_c \approx -25$ eV. It should be noted that \hat{X} is not included in the commonly used Δ SCF procedure. In second order the core-ionization potential obtained within the Δ SCF scheme is given by Eq. (18b).^{22,23}

To gain some further understanding of the difference between Eq. (15) and Eq. (17) we consider in the following a simple model. In this model we put $H_v = \sum_i \epsilon_i a_i^\dagger a_i$ where the summation is over only one doubly occupied orbital φ_o and one doubly unoccupied orbital φ_u . In addition we do not consider doubly excited configurations. The configurations space of the matrix \mathcal{H} includes $|\Psi_0^{Nv}\rangle$ and all the configurations

$$a_{\alpha}^\dagger a_{\beta} | \Psi_0^{Nv} \rangle; \quad \alpha, \beta = \uparrow, \downarrow.$$

The resulting submatrix A_1 is

$$\begin{pmatrix} -\epsilon_c & -V_{ocuc} & -V_{ocuc} + V_{occu} & V_{occu} \\ -V_{ocuc} & -\epsilon_c + \Delta & 0 & -V_{occo} \\ -V_{ocuc} + V_{occu} & 0 & -\epsilon_c + \Delta + V_{uccu} - V_{occo} & V_{uccu} \\ V_{occu} & -V_{occo} & V_{uccu} & -\epsilon_c + \Delta + V_{uccu} \end{pmatrix}, \quad (19)$$

where $\Delta = (\epsilon_u - V_{ucuc}) - (\epsilon_o - V_{occo})$ and E_0^N has been subtracted from all diagonal elements. The eigenvalues of this matrix give the energies of the main and satellite lines in the core spectrum. Equation (15) gives the exact spectrum within the model. Calculating the spectrum via Eq. (17) is, on the other hand, equivalent to solving the eigenvalue problem for the 3×3 matrix which is obtained from (19) by omitting the fourth column and row. At a first glance one may assume that the exact spectrum exhibits four lines while the one calculated via Eq. (17) shows only three lines. This is, however, not the case and both calculated spectra contain three lines. When coupling three electrons to $S_z = \frac{1}{2}$ one obtains only two states with $S = \frac{1}{2}$ and one state with $S = \frac{3}{2}$. The latter state does not acquire intensity.

The two components of a particle-hole excitation with $S = \frac{1}{2}$ usually have a small energy separ-

ation. Their total intensity and their common energy location in the core-hole spectrum are well described by the formula (17). Their individual intensities and relative energy depend, often sensitively, on properties of \hat{X} .

IV. DIAGRAMMATIC EXPANSION OF THE SPECTRUM

A. General

It has already been mentioned in Sec. III that the core-hole spectrum is proportional to the imaginary part of the core-hole Green's function $G_{cc}(\omega)$. The Green's function can be expanded in terms of the interactions V_{mns} and v_{mn} and it is very convenient to describe this expansion in terms of diagrams. The diagrammatic expansion used here is well known and is found in many textbooks.^{19,20} Therefore, we shall not go into the details of the method and only summarize briefly the

rules for handling the diagrams.

The pictorial symbols we use to represent the quantities needed in the diagrammatic procedure are shown in Fig. 1. A straight line pointing upward (from t' to $t > t'$) is called a particle line and a straight line pointing downward (from t' to $t < t'$) is called a hole line. These lines represent the Green's functions.

$$G_{mm'}^o(t, t') = ie^{-i\epsilon_m(t-t')} \delta_{mm'} \begin{cases} -1, & t > 0, n_m = 0 \\ 1, & t \leq 0, n_m = 1. \end{cases} \quad (20)$$

The diagrams representing the n th order of the expansion of G are obtained by drawing all topologically nonequivalent linked diagrams having n wiggly lines $-i(V_{mnsr} - V_{mnr s})$ and $(2n+1)$ iG^o lines. The elements of one kind can be connected only with elements of the other kind. All diagrams which contain iG^o lines which start and end at the same wiggly line should be omitted. Using the HF basis, these diagrams are canceled exactly¹⁹ by the terms which include the matrix elements v_{mn} . The rules to evaluate a given diagram are (i) multiply the contributions of the wiggly lines and of the iG^o lines, (ii) integrate over the intermediate times and sum over the intermediate indices, (iii) multiply the result by the factor $2^{-q}(-1)^L$, where q is the number of permutations of two iG^o lines in the diagram leaving the diagram unchanged and L is the number of loops in the diagram.

The diagrams of $G(t, t')$ for $t \leq t'$ are shown in Fig. 2 up to the third order in the interaction. The analogous diagrams for $t > t'$ can easily be drawn. When using our Hamiltonian H_{cv} in (3) instead of the full Hamiltonian (1), the number of diagrams reduces considerably and the number of summation indices decreases. Since the external indices of each diagram of G_{cc} are core indices and H_{cv} commutes with \hat{N}_c , the time level t_1 at the end of each core line $iG_{cc}^o(t_1, t_2)$ must be the time level at the beginning of the next core line $iG_{cc}^o(t_3, t_1)$; i.e., the two external core lines are

$$(-1) \sum_{k, l, \alpha} (-i)^2 (V_{c\uparrow kc\alpha l} - V_{c\uparrow klc\alpha})^2 \int_{t'}^{t''} dt_1 \int_{t'}^{t_1} dt_2 iG_{c\uparrow c\uparrow}^o(t, t_2) iG_{c\alpha c\alpha}^o(t_2, t_1) iG_{ll}^o(t_2, t_1) iG_{kk}^o(t_1, t_2) iG_{c\uparrow c\uparrow}^o(t_1, t').$$

In the second example we have four possibilities to construct diagrams having four successive core lines. The resulting four contributions are all equal and the final result is shown in the third line in Fig. 3. The last line in this figure exhibits an example where two different contributions arise from one diagram. While one of them possesses two intermediate core lines the other contribution has only one. We see that compared to the general case of expanding G_{cc} using H in (1),

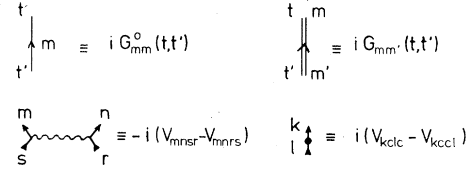


FIG. 1. The definition of the symbols used in the diagrammatic expansion of the Green's function.

connected by $(n-1)$ or less core lines, one at a time. Keeping in mind that $G_{cc}^o(t, t') = 0$ for $t > t'$, all the diagrams of $G_{cc}(t, t')$ vanish for $t > t'$ as does $G_{cc}(t, t')$ itself:

$$G_{cc}(t, t') = 0 \text{ for } t > t'.$$

Moreover, all the diagrams of $G_{cc}(t, t')$ for $t \leq t'$ vanish for which two or more core lines are available at any intermediate time t_i . Consequently, the second diagram of second order, the fourth and sixth diagrams of third order, and the last six diagrams of third order shown in Fig. 2 should not be considered. Finally we should like to mention that when the Green's functions are evaluated with the Hamiltonian (3), the functions G_{sr} are equal to zero if one of r and s represents a valence and the other index a core orbital.

The only diagrams in n th order which contribute to $G_{c\uparrow c\uparrow}$ ($=G_{c\uparrow c\uparrow}$) calculated with H_{cv} are those which contain $(n+1)$ or less successive core lines $iG_{c\alpha c\alpha}^o$ ($\alpha = \uparrow, \downarrow$). No additional core lines are allowed. The existence of the intermediate core lines must be taken explicitly into account when evaluating these diagrams. Let us consider the examples shown in Fig. 3. In the diagram of second order there are two hole lines marked m and n which are between the external core lines. It follows that either n or m must be equal to c and two contributions result. Since the m and n lines are equivalent, we can replace one of them by c and multiply the diagram by a factor of 2. The diagram of second order thus reads

the number of summation indices is reduced here by 1, 2, and 1-2 in the first, second, and third example, respectively.

If the spin-flip operator F_{cv} in (3) is neglected, the occupation number operators $\hat{n}_{c\uparrow}$ and $\hat{n}_{c\downarrow}$ commute with H_{cv} and the rules to handle the diagrams simplify slightly. The external core lines always have the same spin index as the Green's function to be calculated. In case $F_{cv} \neq 0$ the spin index of any intermediate core line takes both \uparrow and \downarrow val-

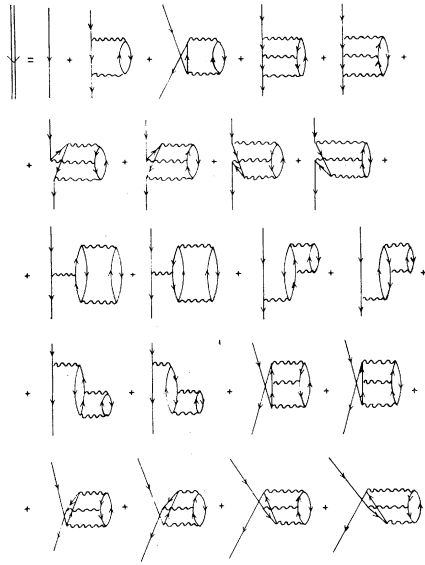


FIG. 2. The diagrams of $G_{cc}(t, t')$ for $t' > t$ up to third order. The second diagram of second order, the fourth and sixth diagrams of third order, and the last 6 diagrams vanish if H_{cv} in (3) is considered.

ues. For $F_{cv} = 0$ all the intermediate core lines have the same spin index as the external lines. In the cases shown in Fig. 3, for example one must put $\alpha = \beta = \uparrow$.

B. A linked-cluster theorem

We have seen that the expansion of the core-hole spectrum (17) includes only diagrams with successive core lines all having the same spin index as the external core lines. We may, therefore, omit the spin index unambiguously in the following. The expression for each diagram contains a product of free-core Green's functions of the type

$$iG_{cc}^o(t, t_1)iG_{cc}^o(t_1, t_2) \cdots iG_{cc}^o(t_{m-1}, t_m)iG_{cc}^o(t_m, t'),$$

which is easily seen to be equal to $(-i)^{2m+3}G_{cc}^o(t, t')$. This fact allows the decoupling of each diagram into a product of a $G_{cc}^o(t, t')$ line and a remaining skeleton. The wiggly lines representing $-i(V_{mccn} - V_{mccn'})$ can now be replaced by a two-indexed quantity, e.g., the interaction point shown in Fig. 1. This procedure is shown in Fig. 4 for a few diagrams.

The sum of all diagrams is clearly given by the sum of all the skeletons multiplied by a free-core line. We may differentiate between linked and unlinked skeletons. It is possible to show that the sum over all skeletons is equal to $\exp(\text{sum of all linked diagrams})$. The proof of this linked-cluster theorem is sketched in Fig. 5 for a simple case. A rigorous analytic proof of this linked-cluster

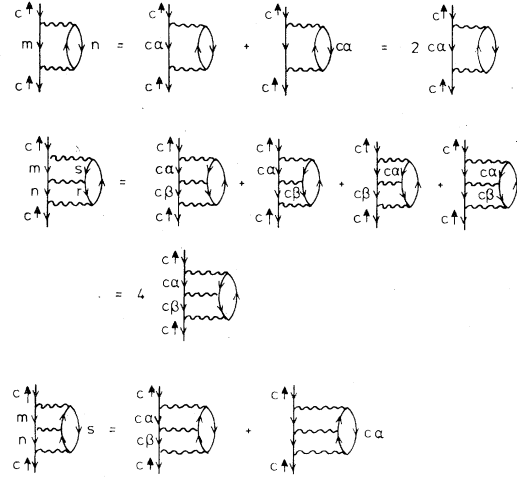


FIG. 3. Three examples of the evaluation of diagrams of the core-hole Green's function $G_{c'c't}$ via H_{cv} in (3). α and β denote spin summation indices.

theorem is given in Appendix A. According to this theorem the core-hole Green's function reads

$$G_{cc}(t) = G_{cc}^o(t)e^{C(t)} = i\Theta(-t)e^{-t\epsilon_c t}e^{C(t)}, \quad (21)$$

where use has been made of the fact that $G_{cc}(t, t')$ depends only on $t - t'$ and is thus a function of a single time variable. In n th order of the interaction the function $C(t)$ contains all linked topologically nonequivalent diagrams with $n_1 (\geq 1)$ interaction points and $n_2 = n - n_1$ wiggly lines connected by $(2n - n_1) iG^o$ (valence) lines. As already pointed out above, diagrams which have $iG^o(t_i, t_i)$ lines should be omitted.

The rules to evaluate a given diagram of $C(t)$ are (i) multiply the contributions of the wiggly lines, the interaction points and the iG^o lines, (ii) integrate over all times and sum over all (valence) indices, (iii) multiply the result by the factor $2^{-q}(-1)^{L+n_1}$. It can be seen from the proof of the linked-cluster theorem in Appendix A that care must be taken when integrating over the times. The wiggly lines and the interaction

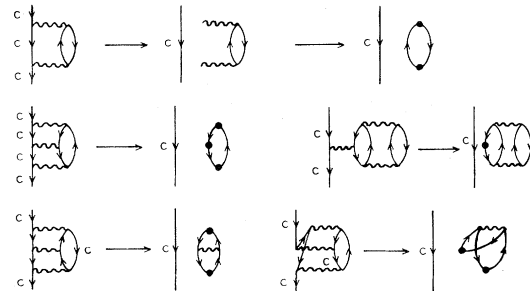


FIG. 4. The decoupling of the contributing diagrams.

points must be treated differently. Whereas the time level of a wiggly line is, in principle, between $-\infty$ and $+\infty$, the time level of an interaction point is between the external times t and 0. The following two examples should clarify the difference. The analytic expressions for the last two diagrams of $C(t)$ shown in Fig. 4 are

$$-i \sum_{i,j,l,k} (V_{iikj} - V_{iljk})(V_{jcic} - V_{jcci})(V_{kcic} - V_{kcci}) \int_t^0 dt_1 \int_t^{t_1} dt_2 \int_t^{t_2} dt_3 G_{kk}^o(t_2 - t_1) G_{ii}^o(t_1 - t_2) G_{ii}^o(t_3 - t_2) G_{jj}^o(t_2 - t_3)$$

and

$$i \sum_{i,j,l,k} (V_{iklj} - V_{ljkj})(V_{jcic} - V_{jcci})(V_{lckc} - V_{lckk}) \times \int_t^{\infty} dt_1 \int_t^{t_1} \Theta(-t_2) dt_2 \int_t^{t_2} dt_3 G_{kk}^o(t_2 - t_1) G_{ii}^o(t_1 - t_2) G_{ii}^o(t_3 - t_1) G_{jj}^o(t_1 - t_3),$$

respectively. As can be seen from the integrals, $t_1 \geq t_2 \geq t_3$ and thus i and k refer to occupied spin orbitals. It is often useful to rewrite the integrals in the latter expression to give

$$\int_t^0 dt_1 \int_t^{t_1} dt_2 \int_t^{t_2} dt_3 + \int_0^{\infty} dt_1 \int_t^{t_1} dt_2 \int_t^{t_2} dt_3 \quad \text{or} \quad \int_t^0 dt_3 \int_{t_3}^0 dt_2 \int_{t_2}^0 dt_1.$$

The analytical expression for $C(t)$ reads [see Eqs. (A10)–(A12)]

$$C(t) = \sum_{n=0}^{\infty} \frac{(-i)^n}{n!} \int_{-\infty}^{\infty} dt_1 \cdots \int_{-\infty}^{\infty} dt_n \{ \langle \Phi_0^{Nv} | T[\bar{V}(t_1)\bar{V}(t_2) \cdots \bar{V}(t_n)] \Phi_0^{Nv} \rangle - \langle \Phi_0^{Nv} | T[\bar{V}_v(t_1)\bar{V}_v(t_2) \cdots \bar{V}_v(t_n)] \Phi_0^{Nv} \rangle \}_{c, |} \quad (22)$$

where $|\Phi_0^{Nv}\rangle$ is the ground-state eigenfunction of $H_0 = \sum_i \epsilon_i \hat{n}_i$ and the valence potential follows from

$$H_v = H_0 + V_v. \quad (23a)$$

Furthermore we define

$$\bar{V}(t_i) = \bar{V}_v(t_i) + \bar{V}_1(t_i) \Theta(-t_i) \Theta(t_i - t), \quad \bar{X}(t_i) = e^{iH_0 t_i} X e^{-iH_0 t_i} \quad (23b)$$

with

$$V_1 = - \sum_{k,l} (V_{kcic} - V_{kcci}) (a_k^\dagger a_l - n_k \delta_{kl}). \quad (23c)$$

Let us briefly interpret this result. The first term in Eq. (22) gives rise to all connected diagrams [indicated by the subscript c at the end of (22)] which are due to the potential V_v of the valence electrons and the potential V_1 , which is equal, up to a constant, to the core-valence interaction term W_{cv} in the presence of a single core hole. In order to obtain $C(t)$ we have to subtract from these diagrams all the connected diagrams which are due to V_v alone. The time dependence of the exponential $C(t)$ is solely determined by the dependence of $\bar{V}(t_i)$ on t as shown in Eq. (23b).

If we neglect the interaction between the valence electrons, i.e., $V_v = 0$, the function $C(t)$ simply becomes

$$C(t) = \sum_{n=0}^{\infty} \frac{(-i)^n}{n!} \int_t^0 dt_1 \int_t^0 dt_2 \cdots \int_t^0 dt_n \langle \Phi_0^{Nv} | T[\bar{V}_1(t_1)\bar{V}_1(t_2) \cdots \bar{V}_1(t_n)] \Phi_0^{Nv} \rangle_c. \quad (24)$$

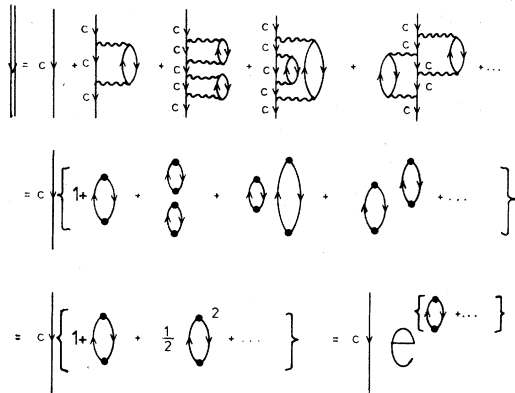


FIG. 5. On the linked-cluster theorem.

In n th order this function includes all connected diagrams which can be drawn from n interaction points and n free Green's-function lines via the rules discussed above. Equation (24) is essentially equivalent to the result obtained by Nozières and DeDominicis²⁴ in their discussion of x-ray singularities in metals. Interestingly, the linked-cluster theorem (21) is also valid if the valence electrons are allowed to interact with each other.

The derivatives of $C(t)$ with respect to t determine the moments of the spectrum. The m th moment M_m of the core-hole spectrum is defined by

$$M_m \equiv \int (\omega - \epsilon_c)^m P(\omega) d\omega. \quad (25a)$$

It is easily shown with the aid of Eq. (21) that

$$M_m = |\tau|^2 i^m \frac{\partial^m}{\partial t^m} e^{C(t)} \Big|_{t=0}, \quad (25b)$$

where $|\tau|^2$ is the proportionality constant of Eq. (12). An additional relation can be derived from Eq. (17):

$$M_m = |\tau|^2 \langle \Psi_0^N v | \left(\sum_{i,j} (V_{icjc} - V_{icjf}) \times [a_i^\dagger a_j - n_i \delta_{ij}] \right)^m | \Psi_0^N v \rangle. \quad (25c)$$

The total intensity of the spectrum is equal to the zeroth moment $M_0 = |\tau|^2 \exp[C(0)] = |\tau|^2$ which does not depend on the electron-electron interaction. All higher moments depend on the interaction between the valence electrons. The center of gravity of the core-hole spectrum is given by $\epsilon_c + M_1/M_0$. If only relaxation effects are considered in the calculation of the spectrum, the first moment vanishes and the center of gravity is equal to the HF orbital energy ϵ_c (see Sec. IV C). Taking correlation effects into account implies that $M_1 \neq 0$ and the center of gravity deviates from ϵ_c . The diagrams of $C(t)$ which contribute to M_1 are those which have only a single interaction point. This can be seen from Eq. (25b). After taking the derivative with respect to t , all diagrams of $C(t)$ which have more than one interaction point yield integrals of the type \int_t^0 which vanish for $t \rightarrow 0$. The lowest-order diagrams which contribute to M_1 are those third-order diagrams which correspond to energy-independent diagrams of the self-energy part^{19,20} $\Sigma_{cc}(\omega)$ of the core Green's function $G_{cc}(\omega)$. It has been shown explicitly by Born *et al.*²³ that these diagrams do not appear in the expansion of the spectrum within the Δ SCF scheme. To make further contact with the self-energy part $\Sigma_{cc}(\omega)$ we consider Eq. (3.28a) in Ref. 18 and obtain

$$M_1/M_0 = \Sigma_{cc}(\infty). \quad (26)$$

The term $\Sigma_{cc}(\infty) = \lim_{\omega \rightarrow \infty} \Sigma_{cc}(\omega)$ is equal to the sum of all diagrams of the self-energy part which are independent of energy ω . It constitutes a statical correlation potential which leads to a shift of the center of gravity of the core-hole spectrum. Calculations reveal that $\Sigma_{cc}(\infty)$ is fairly small for H_2O and CH_4 (≈ 0.1 eV) but large for N_2 (≈ 1 eV).

The Dyson equation^{19,20} which relates the Green's functions to the self-energy part is commonly used as a starting point in the calculation of G . Instead of expanding G directly, the self-energy part is expanded in terms of the interaction matrix elements. In this way any diagram of the self-energy part leads to an infinite number of diagrams

of G . In the core case the Dyson equation reads

$$G_{cc}(\omega) = [\omega - \epsilon_c - \Sigma_{cc}(\omega)]^{-1}. \quad (27)$$

Now the question arises whether the Dyson equation approach or the approach via the linked-cluster formula (21) is more suitable for evaluating the Green's function. Clearly, a linked-cluster theorem of the present type does not apply to the Green's functions of valence electrons. In this case the Dyson equation is very useful at least for electrons near the Fermi level, where the quasiparticle properties of G are well-reproduced even with a low-quality self-energy part.²⁵ Furthermore, the Dyson equation allows the treatment of correlation and relaxation effects on the same level of accuracy which is important for valence electrons.¹⁸ For core levels, on the other hand, the relaxation effects are dominant and Eq. (21), which has been derived using genuine properties of core orbitals, represents the more appealing starting point. Calculating the core Green's function via the Dyson equation (27) with $\Sigma_{cc}(\omega)$ expanded up to the lowest contributing order often leads to useful results for the main line in the spectrum.²⁶ The shake-up energies obtained are, however, of an extraordinarily low accuracy, since they have not been determined in the field of the relaxed core hole. Computing the Green's function from the linked-cluster equation (21) with $C(t)$ expanded up to the lowest contributing order leads to drastically improved shake-up energies (for more details see Sec. V).

C. The Δ SCF procedure

The Δ SCF procedure has been widely used to compute the energies and the relative intensities of the main and satellite² lines of core-hole spectra of atoms and molecules. It is, therefore, interesting to find out which of the diagrams of G_{cc} constitute the Δ SCF procedure or, more precisely, which diagrams describe relaxation processes only. Born *et al.*²³ have derived an expression for the ionization potential $I(\Delta\text{SCF})$ obtained within the Δ SCF scheme by expanding $I(\Delta\text{SCF})$ up to third order in the perturbation. They have also shown which of the diagrams of $\Sigma_{cc}(\omega)$ of second and third order correspond to the resulting $I(\Delta\text{SCF})$. Their investigation has been helpful to us in generalizing the results to higher orders.

First of all it should become clear that we may use the linked-cluster equation (21) because the Δ SCF scheme does not incorporate the spin-flip term F_{cv} . On the other hand, the Δ SCF procedure includes terms not accessible with H_{cv} in (3).

These terms are of the form $V_{ctc+ctk}/(\epsilon_c - \epsilon_k)$, where k denotes a virtual orbital, and are negligible.

In the simple case where $V_v=0$ (see Eq. 23a), each diagram of $C(t)$ forms a loop of interaction points connected by valence lines iG^0 . Examples for such loops are shown in Fig. 6(a). Equation (23c) implies that $C(t)$ does not contain a diagram with a single interaction point. Since there is no correlation between the electrons, all the diagrams of $C(t)$ with $V_v=0$ describe relaxation effects and are included in the Δ SCF scheme. There are many additional kinds of diagrams of $C(t)$ when $V_v \neq 0$, some of which still describe relaxation effects. To distinguish between these diagrams and those which describe correlation effects, we apply the following simple procedure. Remove all wiggly lines and, if necessary, straighten the iG^0 lines connecting interaction points in a given diagram. If the resulting structure is a regular loop diagram of $C(t)$ with $V_v=0$, the original diagram is included in the Δ SCF scheme. The procedure is exemplified in Fig. 6(b). In Fig. 6(c) all the third-order diagrams of $C(t)$ are shown which are included in the Δ SCF procedure. The only diagrams of third order which describe correlation effects are those which exhibit a single interaction point. Since all the diagrams which have a single interaction point are not included in the Δ SCF scheme, it follows from Eq. (26) that

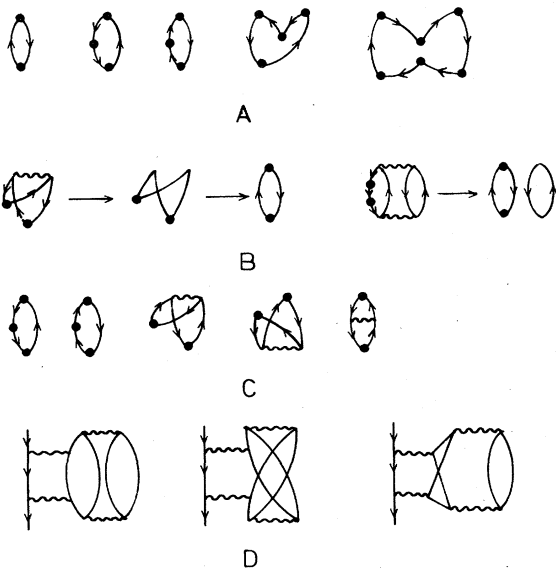


FIG. 6. (a) Diagrams belonging to $C(t)$ with $V_v=0$; (b) examples for the procedure to distinguish between correlation and reorganization diagrams of $C(t)$; (c) the diagrams of third order which are included in the Δ SCF scheme; (d) some Green's function diagrams not included in the Δ SCF scheme.

$$M_1/M_0=0$$

and hence the center of gravity of a core-hole spectrum calculated with the Δ SCF procedure is simply given by ϵ_c . Some additional correlation diagrams of fourth order are depicted in Fig. 6(d).

D. An illustrative example

The main objective of this subsection is to calculate exactly via diagram summation the core-hole spectrum for the following simple model Hamiltonian

$$H_{cv} = \sum_{\alpha} (\epsilon_c \hat{n}_{c\alpha} + \epsilon_o \hat{n}_{o\alpha} + \epsilon_u \hat{n}_{u\alpha}) - V \sum_{\alpha, \beta} (1 - \hat{n}_{c\alpha}) (a_{o\beta}^{\dagger} a_{u\beta} + a_{u\beta}^{\dagger} a_{o\beta}), \quad (28)$$

which describes the interaction of three spatial orbitals, a core orbital φ_c , an occupied valence orbital φ_o , and an unoccupied orbital φ_u . There are many ways to calculate the corresponding core-hole spectrum. Since the configurational space is very limited, the configuration interaction approach to Eq. (17) is the most efficient one. Choosing the valence configurations

$$|1\rangle = |\Psi_0^{Nv}\rangle, \\ |2\rangle = 2^{-1/2} (a_{u\uparrow}^{\dagger} a_{o\uparrow} + a_{u\downarrow}^{\dagger} a_{o\downarrow}) |\Psi_0^{Nv}\rangle,$$

and

$$|3\rangle = a_{u\uparrow}^{\dagger} a_{u\downarrow}^{\dagger} a_{o\uparrow} a_{o\downarrow} |\Psi_0^{Nv}\rangle,$$

one immediately arrives at the matrix

$$A = \begin{bmatrix} -\epsilon_c & -\sqrt{2} V & 0 \\ -\sqrt{2} V & -\epsilon_c + \Delta & -\sqrt{2} V \\ 0 & -\sqrt{2} V & -\epsilon_c + 2\Delta \end{bmatrix},$$

where Δ denotes the particle-hole excitation energy $\epsilon_u - \epsilon_o$. The core Green's function is simply given by $(\omega - A)_{1,1}^{-1}$ and the core-hole spectrum reads

$$P(\omega) \sim \frac{(\Delta + a)^2}{4a^2} \delta(\omega - \epsilon_c + \Delta - a) + \frac{(\Delta - a)^2}{4a^2} \delta(\omega - \epsilon_c + \Delta + a) + \frac{2V^2}{a^2} \delta(\omega - \epsilon_c + \Delta), \quad (29)$$

where $a = (\Delta^2 + 4V^2)^{1/2}$.

As we shall see below, a much larger effort is required to derive Eq. (29) using diagrammatic techniques. This is not at all surprising. It is well known that the diagrammatic solution of even a "two-state" problem is extremely complicated compared to the quadratic equation arising in the configuration-interaction approach. The diagrammatic approach has been designed to solve approximately "many-states" problems for which brute force configuration-interaction methods

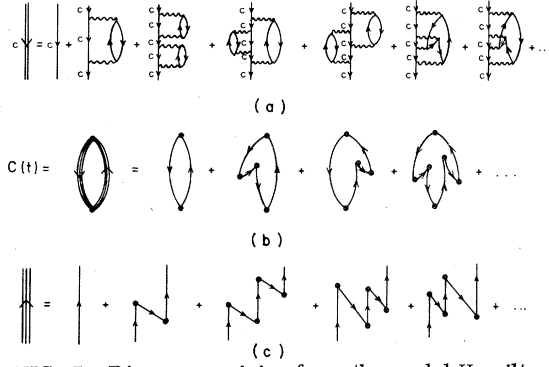


FIG. 7. Diagrams arising from the model Hamiltonian (28). (a) The diagrams of the core Green's function shown up to fourth order; (b) the diagrams of $C(t)$; (c) the diagrams of the auxiliary function used to construct $C(t)$.

are more tedious, more difficult to interpret, or even inapplicable as for, e.g., infinite electronic systems.

The diagrams of G_{cc} are shown in Fig. 7(a), where all the diagrams up to fourth order are shown explicitly. The diagrams have a number of properties in common: an even number of wiggly lines, a particle and a hole valence line emerge from one vertex, and two core-hole lines from the other vertex of every wiggly line. From these diagrams the diagrams of the exponential function $C(t)$ are easily obtained. They are depicted in Fig. 7(b). Every interaction point is associated with one particle and one hole line. We may visualize $C(t)$ as two auxiliary Green's functions ρ_u and ρ_o , the first pointing upwards and the second downwards, connected by two interaction points [see Fig. 7(b)]. The diagrams belonging to ρ_u are shown in Fig. 7(c) and the diagrams of ρ_o are obtained by turning these diagrams upside down. The exponential function $C(t)$ now reads (see the rules to evaluate diagrams in Sec. IV B)

$$C(t) = -2V^2 \int_t^0 dt_1 \int_t^{t_1} dt_2 \rho_o(t_2 - t_1) \rho_u(t_1 - t_2), \quad (30)$$

where the factor 2 is due to the summation over the spin.

The calculation of $\rho_u(t)$ is not as simple as it may seem at first glance, because all the interaction points of a diagram of ρ_u are confined to times \bar{t} with $0 \leq \bar{t} \leq t$. To determine ρ_u we investigate the analytic expressions corresponding to its diagrams and recognize that a function $\rho_u(t, t')$ closely related to $\rho_u(t)$ is subject to the recursion relation

$$\rho_u(t, t') = G_{uu}^o(t) + V^2 \int_0^t dt_1 \int_{t_1}^{t'} dt_2 G_{uu}^o(t - t_1) \times G_{oo}^o(t_1 - t_2) \rho_u(t_2, t'). \quad (31a)$$

The auxiliary function is obtained from $\rho_u(t) = \lim_{t' \rightarrow t} \rho_u(t, t')$, and the function $\rho_o(t)$ is determined according to the relation

$$\rho_o(t) = -\rho_u(-t). \quad (31b)$$

The integral equation (31a) is easily converted into the linear differential equation

$$\ddot{\rho}_u + i(\epsilon_o + \epsilon_u) \dot{\rho}_u + (V^2 - \epsilon_o \epsilon_u) \rho_u = 0,$$

which has the general solution

$$\rho_u(t, t') = e^{-i(\epsilon_o + \epsilon_u)t/2} \times [K_1(t') e^{iat/2} + K_2(t') e^{-iat/2}].$$

The coefficients K_1 and K_2 are determined by inserting the latter expression into the integral equation (31a). The final result reads

$$\begin{aligned} \rho_u(t) &= \lim_{t' \rightarrow t} \rho_u(t, t') \\ &= i2a e^{-i(\epsilon_o + \epsilon_u)t/2} \\ &\quad \times [(a + \Delta) e^{iat/2} + (a - \Delta) e^{-iat/2}]^{-1}. \end{aligned} \quad (32a)$$

The exponential function $C(t)$ is now obtained by elementary integration of Eq. (30)

$$C(t) = i\Delta t + 2 \ln[\cos(at/2) - i(\Delta/a) \sin(at/2)]. \quad (32b)$$

Using the general formula

$$P(\omega) \sim \int_{-\infty}^{\infty} dt e^{i(\omega - \epsilon_c)t} e^{C(t)}, \quad (33)$$

we finally recover the exact core-hole spectrum (29).

V. THE BOSON APPROXIMATION

A. Theory

The exact self-energy part of the core Green's function $G_{cc}(\omega)$ calculated with the Hamiltonian (3) has the following spectral representation:

$$\Sigma_{cc}(\omega) = \Sigma_{cc}(\infty) + \sum_n \frac{|X_n|^2}{\omega - y_n - i0^+}. \quad (34)$$

For $t \leq 0$ this relation leads to the identity

$$\begin{aligned} \Sigma_{cc}(t) &= G_{cc}^o(t) \left(-i \Sigma_{cc}(\infty) \delta(t) \right. \\ &\quad \left. + \sum_n |X_n|^2 e^{i(\epsilon_c - y_n)t} \right). \end{aligned} \quad (35)$$

The diagrams in the expansion of the first term in the parentheses correspond to those diagrams of $C(t)$ with a single interaction point. The diagrams included in the expansion of the second term in the parentheses of (35) contain all the other diagrams of $C(t)$, but, in addition, also unlinked diagrams contained in $\exp[C(t)]$. An example which illustrates the procedure to obtain an unlinked diagram is shown in Fig. 8. If

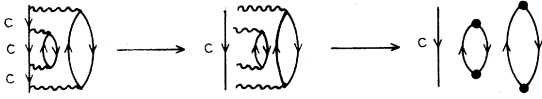


FIG. 8. The decomposition of a diagram of the self-energy part into a product of G_{cc}^0 and an unlinked diagram of $\exp[C(t)]$.

we consider an approximation of $\Sigma_{cc}(\omega)$ which does not lead to unlinked diagrams, it may not have a spectral representation. Many useful approximate self-energy parts have, however, a spectral representation equivalent to the one in (34) and do not lead to unlinked diagrams. Since all the diagrams of these approximate self-energy parts correspond to diagrams of $C(t)$, we may calculate the latter function using the relation

$$C(t) = - \int_t^0 dt_2 \int_t^{t_2} dt_1 \Sigma_{cc}(t_1 - t_2) \times [G_{cc}^0(t_1 - t_2)]^{-1}. \quad (36)$$

The resulting Green's function $G_{cc}(t) = ie^{-t\epsilon_c t} \times e^{C(t)}$ includes infinitely more diagrams than the Green's function calculated from the approximate self-energy part Σ_{cc} via the Dyson equation (whenever unambiguous we use the same notation for the approximate and exact quantities). With the aid of Eq. (35) we obtain

$$C(t) = -i\Sigma_{cc}(\epsilon_c)t + \sum_n \frac{|X_n|^2}{(\epsilon_c - y_n)^2} (e^{i(\epsilon_c - y_n)t} - 1). \quad (37)$$

The corresponding core-hole spectrum is easily determined from Eq. (33). If we consider only one pole of $\Sigma_{cc}(\omega)$, the spectrum reads

$$P_n(\omega) \sim e^{-a_n} \sum_{m=0}^{\infty} \frac{a_n^m}{m!} \delta(\omega - \epsilon_c - \Sigma_{cc}(\epsilon_c) - m\Omega_n), \quad (38)$$

where $a_n = |X_n|^2 / (\epsilon_c - y_n)^2$ and $\Omega_n = y_n - \epsilon_c$. The complete spectrum is obtained by convoluting the individual spectra.

A Poisson distribution as in Eq. (38) can also be derived for a system of bosons which are coupled to a single hole. If we calculate^{4a,18} the core-hole spectrum (12) using the boson Hamiltonian

$$H_{cb} = \tilde{\epsilon}_c \hat{n}_c + \sum_n \Omega_n (b_n^\dagger b_n + \frac{1}{2}) + (1 - \hat{n}_c) \sum_n \kappa_n (b_n + b_n^\dagger), \quad (39)$$

where b_n is an annihilation operator for a boson

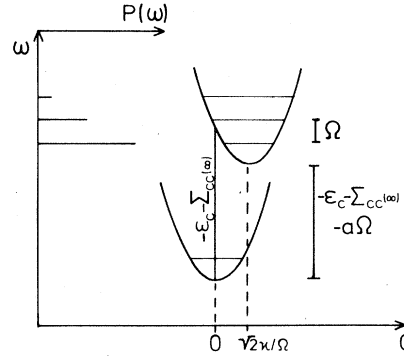


FIG. 9. A schematic drawing illustrating the physical situation suggested by Eq. (38).

with frequency Ω_n , we simply recover the spectra (38) and (37) with $a_n = (\kappa_n / \Omega_n)^2$, $\tilde{\epsilon}_c = \epsilon_c + \Sigma_{cc}(\infty)$, and $\Sigma_{cc}(\epsilon_c) - \Sigma_{cc}(\infty) = \sum_n a_n \Omega_n$. One may, therefore, refer to the approximation (37) for $C(t)$ as the boson approximation. Equations (38) and (37) suggest that the core-ionization process can be visualized as follows. In its neutral state the system is schematically described by a harmonic multidimensional potential energy surface. In its core-ionized state the system is described by the same surface shifted by $\sqrt{2} \kappa_n / \Omega_n$ in each direction of the abstract dimensionless bosonic space $\vec{Q} = (Q_1, Q_2, \dots, Q_n, \dots)$, where $Q_n = (b_n + b_n^\dagger) / \sqrt{2}$. The vertical energy difference between the initial and final surfaces at $Q=0$, which is the position of the minimum of the initial surface, is equal to $\epsilon_c + \Sigma_{cc}(\infty)$. Ejecting a core electron now results in the excitations from the ground state of the initial potential-energy surface to all possible states of the final surface and the intensity distribution is governed by the well-known Franck-Condon principle. This analogy with the Franck-Condon principle has already been noted by Manne and Åberg.³⁷ The situation is illustrated in Fig. 9 for the simple one-dimensional case. The center of gravity of the spectrum (38) is $\epsilon_c + \Sigma_{cc}(\infty)$ and is, thus, formally equal to the exact result (26).

In order to gain understanding of the meaning of the quantities appearing in Eqs. (37) and (38) we briefly compare with the lowest-order term in the expansion of $\Sigma_{cc}(\omega)$:

$$\Sigma_{cc}(\omega) = \sum_{j,l} \frac{(V_{jcl} - V_{lcc})^2}{\omega - \epsilon_c + \epsilon_j - \epsilon_l} n_j (1 - n_j). \quad (40)$$

The quantity $I_c = -\epsilon_c - \Sigma_{cc}(\epsilon_c)$ is the core-ionization potential obtained in second order [see Eq. (18b)]. $-\Sigma_{cc}(\epsilon_c)$ may generally be referred to as the relaxation shift of the ionization potential $-\epsilon_c$ of the noninteracting HF particles. The frequencies of the harmonic oscillators are, in

zeroth order, given by $\Omega_{jl} = \epsilon_j - \epsilon_l$, where j and l denote an unoccupied and an occupied spin orbital, respectively. When comparing with more sophisticated self-energy parts,²⁷ one finds in first order the following expression for the harmonic frequencies (exchange is neglected):

$$\Omega_{jl} = (\epsilon_j - V_{jclc}) - (\epsilon_l - V_{lclc}) - V_{jljl}. \quad (41)$$

This equation is easily interpreted. Due to the presence of a core hole a valence orbital energy ϵ_m is shifted in first order by V_{mcmc} . Thus, the Ω_{jl} are simply excitation energies of the core-ionized system, i.e., the Ω_{jl} are shake-up energies. The Poisson parameter a_{jl} can usually be written as $(\kappa_{jl}/\Omega_{jl})^2$, where κ_{jl} is the coupling constant in the boson Hamiltonian (39). In first order we find by comparing Eqs. (37) and (40) that $\kappa_{jl} = (V_{jclc} - V_{jcll})$. We may conclude that all the parameters in the boson Hamiltonian can be given a simple interpretation in physical terms.

In the investigations of electronic spectra of processes involving the transition of localized electrons one often meets the situation where a boson approximation is applicable. The probably simplest example is given by plasmon excitations. Although being (collective) electronic excitations, plasmons are known to be bosons. In the case of core-hole ionization in solids a Hamiltonian essentially equivalent to H_{cb} in (39) has been applied by Langreth^{4b} to investigate the plasmon excitations. Mahan points out in his review^{4a} that the three line-broadening mechanisms, phonon and electron excitations in a solid as well as atomic collisions in a gas can be well described by an integral

$$\int_{-\infty}^{\infty} e^{i(\omega - \epsilon_0)t} e^{i\Phi(t)},$$

where $\Phi(t)$ is closely related to our $C(t)$ in Eq. (37); i.e., the boson approximation applies to these cases as well.

The limits of the boson approximation (37) become immediately clear from the structure of the spectrum (38). The spectrum allows for triple and higher excitations between a given occupied spatial orbital and a specific unoccupied spatial orbital. Since these excitations cannot take place in electronic systems where each spatial orbital can contain only two electrons, their probability must be small. In other words, the Poisson parameters a_n must be small and, consequently, the shake-up energies must be large compared to their coupling to the core hole to enable us to apply the boson approximation

$$|X_n| \ll |\epsilon_c - y_n|; \quad |\kappa_n| \ll \Omega_n. \quad (42)$$

Let us now return to the simple model of Sec.

IV D. The exact exponential function $C(t)$ for this model is found in Eq. (32b) and can be written in the following form [$\tilde{\Omega} = (\Omega^2 + 2|X|^2)^{1/2}$]:

$$C(t) = i(\Omega - \tilde{\Omega})t - 2 \ln \left(1 + \frac{\tilde{\Omega} - \Omega}{\tilde{\Omega} + \Omega} \right) + 2 \ln \left(1 + \frac{\tilde{\Omega} - \Omega}{\tilde{\Omega} + \Omega} e^{i\tilde{\Omega}t} \right), \quad (43a)$$

which is suitable for a Taylor expansion. Assuming the condition (42) to be valid, we find in lowest order the boson approximation:

$$C(t) = -i \frac{|X|^2}{\Omega} t + \frac{|X|^2}{\Omega^2} (e^{i\Omega t} - 1). \quad (43b)$$

If we generalize the model of Sec. IV D to include many occupied and unoccupied orbitals, the function $C(t)$ is crudely approximated by

$$C(t) = i \sum_n (\Omega_n - \tilde{\Omega}_n)t - 2 \ln \left(1 + \sum_n \frac{\tilde{\Omega}_n - \Omega_n}{\tilde{\Omega}_n + \Omega_n} \right) + 2 \ln \left(1 + \sum_n \frac{\tilde{\Omega}_n - \Omega_n}{\tilde{\Omega}_n + \Omega_n} e^{i\tilde{\Omega}_n t} \right), \quad (44)$$

where n specifies a possible single particle-hole excitation. This equation implies that the boson approximation cannot be expected to describe accurately the properties of main lines in realistic spectra. The errors inherent to the boson approximation for an excitation specified by n add up for the first two terms of $C(t)$, Eq. (44), but not for the last term which contributes to the relative energies and intensities of the satellite lines. We, therefore, conclude that if the inequality (42) is satisfied, the boson approximation can safely be used to calculate the energies of the satellite lines relative to the main line as well as their relative intensities.

B. Application to H₂O

The core-hole spectrum of the water molecule has been investigated both experimentally²⁸ and theoretically.²⁹⁻³² The experimental spectrum is not sufficiently resolved to allow an unambiguous assignment of the satellite lines contained in it. One must, therefore, rely on theoretical studies in order to obtain a more detailed understanding of the spectrum. We have chosen H₂O as our example because all the satellite lines in the spectrum are weak compared to the main line and the boson approximation should be applicable. Our goal is to demonstrate that the simple bosonic picture leads to shake-up energies and intensities which are as accurate as those obtained by the commonly used approaches. The bosonic picture is, of course, of a limited applicability, but gives us additional insight into the physical process of core

ionization.

According to Sec. VA the self-energy part Σ_{cc} used to construct the exponential function $C(t)$ should not lead to an overcounting of diagrams of $G_{cc}(t) = i \exp[-i\epsilon_c t + C(t)]$. The simplest self-energy part of this kind is the second-order term (40) in the expansion of the exact Σ_{cc} . The results obtained with (40) are generally known to be poor, mainly because of the missing interaction between the orbitals involved in the shake-up process. The simplest self-energy part which takes account of this interaction and consists of an infinite summation of diagrams including the second-order diagram is the so-called $2ph$ -TDA self-energy part.¹⁸ This self-energy part is discussed in detail elsewhere²⁷ for the general case where H in (1) is the appropriate Hamiltonian. The $2ph$ -TDA procedure simplifies considerably when the Hamiltonian H_{cv} in (3) is used. Then, solving the Dyson equation for the core Green's function becomes equivalent to the calculation of G_{cc} using the following ansatz for the ionic states:

$$|\Psi_n^{N-1}\rangle \simeq a_c |\Phi_0^N\rangle + \sum_{k,l,\alpha} \gamma_{kl\alpha}^{(n)} a_k^\dagger a_l a_{c\alpha} |\Phi_0^N\rangle, \quad \alpha = \uparrow, \downarrow \quad (45)$$

where $|\Phi_0^N\rangle$ is the HF ground state and the $\gamma_{kl\alpha}^{(n)}$ are variational parameters. With the aid of Eq. (45) and the Dyson equation an explicit analytic expression for the $2ph$ -TDA self-energy part can be given:

$$\Sigma_{cc}(\omega + \epsilon_c) = (V_1^\dagger, V_2^\dagger) \begin{bmatrix} \omega \underline{1} - \underline{K} - \underline{C}_1 & -\underline{C}_3 \\ -\underline{C}_3^\dagger & \omega \underline{1} - \underline{K} - \underline{C}_2 \end{bmatrix}^{-1} \times \begin{bmatrix} V_1 \\ V_2 \end{bmatrix}, \quad (46)$$

where \underline{K} , \underline{C}_1 , \underline{C}_2 , and \underline{C}_3 are matrices with elements

$$\begin{aligned} K_{lk, l'k'} &= (\epsilon_l - \epsilon_k) \delta_{ll'} \delta_{kk'}, \\ C_{1lk, l'k'} &= (V_{k'c}^\dagger c^\dagger k c^\dagger - V_{k'c}^\dagger c^\dagger k) \delta_{ll'} \\ &\quad + (V_{l'c}^\dagger c^\dagger l c^\dagger - V_{l'c}^\dagger c^\dagger l) \delta_{kk'} \\ &\quad - \frac{1}{2} (V_{kl'k'i} - V_{kl'l'k'}), \\ C_2 &= C_1(\uparrow \leftrightarrow \downarrow), \\ C_{3lk, l'k'} &= V_{k'c}^\dagger c^\dagger k' \delta_{ll'} + V_{l'c}^\dagger c^\dagger l \delta_{kk'}. \end{aligned}$$

V_1 and V_2 are column vectors with elements $V_{1lk} = V_{k'c}^\dagger c^\dagger k c^\dagger - V_{k'c}^\dagger c^\dagger k$ and $V_{2lk} = V_{k'c}^\dagger c^\dagger k$. The dimension of the matrices is relatively small, since l denotes occupied and k unoccupied orbitals and the summation over the spins can be done explicitly.²⁷

We shall see below that the variational ansatz (45)

leads to accurate energies of main lines, but to a very poor description of the satellite lines. The calculated energies of the satellite lines are much too high, since the ansatz does not include higher excitations of the type $a_k^\dagger a_l a_{c\alpha}^\dagger a_i a_c |\Phi_0^N\rangle$. The inclusion of these excitations is necessary to describe the relaxation of the satellite lines. On the other hand, if we calculate the Green's function via the linked-cluster expression using $\Sigma_{cc}(\omega)$ in (46) to construct the exponential function $C(t)$, the final result does include higher excitations. This shows that the linked-cluster equation (21) is more suitable to calculate core spectra than the Dyson equation (27).

It has been pointed out in Sec. IVB that the linked-cluster theorem is strictly valid if the spin-flip term F_{cv} is ignored. The effect of F_{cv} should, if necessary, be considered subsequently. When applying the boson approximation it is, on the other hand, favorable to include the effect of F_{cv} in the self-energy part used to construct the exponential function $C(t)$. In this way the splitting of the satellite lines into doublets predicted by the ansatz (45) is maintained through the entire calculation. The error made in violating the linked-cluster theorem by incorporating F_{cv} into $C(t)$ is negligible compared to the error introduced by the boson approximation itself. Equation (46) simplifies if F_{cv} is put to zero, since both V_2 and C_3 vanish in this case.

As a starting point for the computational procedure an *ab initio* calculation has been performed³³ for H₂O at its experimental geometry using the program system MUNICH.³⁴ The basis set consists of eleven *s*-type and seven *p*-type Gaussian functions for the oxygen atom contracted to five *s*-type and three *p*-type functions. For each hydrogen atom six *s*-type functions have been used contracted to three functions. A $2ph$ -TDA calculation based on H in (1) has been carried out taking into account all occupied orbitals and the thirteen virtual spatial orbitals lowest in energy.³³ In this way we can also investigate the importance of terms not included in H_{cv} . We have found that the shift of the main line owing to the difference between the Hamiltonians (1) and (3) is less than 0.4 eV which has to be compared with the total change of 20 eV of the core-ionization potential. The influence on the shake-up energies is even much less significant. The core-ionization potential obtained with the $2ph$ -TDA Green's function approach is 539.99 eV and is in excellent agreement with the experimental value²⁸ of 539.93 eV. This agreement between theory and experiment is, however, somewhat fortuitous mainly because of the truncation of the orbital basis. The lowest shake-up energy obtained is nearly 20 eV too high

when compared to experiment. If the $2ph$ -TDA self-energy part is used to construct the exponential function $C(t)$, this shake-up energy agrees well with the experimental value.

The shake-up energies and relative intensities obtained for H_2O using the boson approximation are listed in Table I together with the theoretical results of Aarons *et al.*,²⁹ Wood,³⁰ Wahlgren,³² and Svenson *et al.*³¹ There is no accurate agreement between the results obtained with any two methods. However, all the results indicate, in agreement with experiment,²⁸ that (i) there are several satellite lines which acquire intensity, (ii) the satellite line lowest in energy is situated 16–18 eV above the main line (iii) there is an accumulation of satellite intensity at 23–26 eV. The present calculation predicts a great portion of the total satellite intensity to be located above 30-eV shake-up energy. This finding is in agreement with Svenson *et al.* When comparing the calculated satellite intensities with experiment, one should keep in mind that the vibrational broadening can be extremely different for different satellite lines. Furthermore, the use of a finite basis set does not allow a correct description of shake-off processes and the computed high-lying discrete lines may simulate to some extent these processes. This may indeed be the case for the satellite lines situated at relative energies larger than ≈ 30 eV. The intensity of these lines should be thought of as being spread over a larger energy range when compared to experiment. The experimental spectrum exhibits a broad structure between 30 and 40 eV above the main line.

VI. SUMMARY

The core-hole spectrum can, in principle, be determined using the standard formal many-body theory based on the full electronic Hamiltonian.

TABLE I. Calculated energies and intensities of satellite lines in the oxygen core-ionization spectrum of H_2O . All energies (in eV) and intensities (in %) are given relative to the main line.

Present results		Aarons <i>et al.</i> (Ref. 29)		Wood (Ref. 30)		Wahlgren (Ref. 32)		Svenson <i>et al.</i> (Ref. 31)	
Energy	Intensity	Energy	Intensity	Energy	Intensity	Energy	Intensity	Energy	Intensity
17.25	2.0	17.8	3.1	17.6	0.8	17.97	2.3	15.91	0.1
19.27	0.1			22.4	0.3	19.40	1.3	19.77	0.1
20.38	0.2			23.4	0.3	22.09	0.4	19.83	0.3
23.56	6.4	23.8	8.1	25.1	3.5	22.46	0.5	21.22	0.7
27.19	0.4			25.6	1.9	23.45	5.2	21.96	0.9
29.81	0.8			26.9	0.2	24.20	0.1	22.12	0.5
36.34	1.7			27.1	1.2	25.48	2.5	22.93	1.3
37.05	8.7			28.1	0.6	26.04	0.3	24.60	2.0
37.37	2.8			28.4	0.2	27.25	1.3	24.82	2.3
38.14	4.6			28.4	0.6	28.17	0.1	34.73	0.1
39.86	0.3			29.7	0.2	28.90	0.9	36.31	4.0

The theory is, however, simplified considerably when based on a Hamiltonian which has been derived by making explicit use of the genuine properties of core orbitals. The number of terms in the perturbation expansion is then greatly reduced as is the number of the summation indices in each term. Furthermore, the introduction of the core Hamiltonian leads to a useful linked-cluster theorem which relates the core-hole spectrum to an exponential function $C(t)$ for which a diagrammatic expansion is given. The linked-cluster expression $G_{cc}(t) = G_{cc}(t) \exp[C(t)]$ has been found to be superior to the Dyson equation as a starting point to calculate the core-hole spectrum and offers more physical insight into the problem.

Starting from the linked-cluster theorem it has been shown that under certain well-defined conditions the core-hole spectrum is the same as for a system of bosons which are coupled to a single localized hole. This suggests that the core-ionization process can be visualized as a transition between two multidimensional potential-energy surfaces in the abstract bosonic space, the resulting intensity distribution being governed by the well-known Franck-Condon principle. Numerical computations have been performed for the water molecule within the boson approximation, and satisfactory agreement with experiment is found.

ACKNOWLEDGMENTS

The authors are indebted to W. von Niessen for performing the numerical calculations on H_2O , and gratefully acknowledge financial support by the Deutsche Forschungsgemeinschaft.

APPENDIX

In this section we present the analytic proof of the linked-cluster theorem discussed in Sec. IV B. We consider the Hamiltonian (3) without the spin-

flip term

$$H_{cv}(\hat{n}_{c\uparrow}, \hat{n}_{c\downarrow}) = H_v + H_c + W_{cv} \quad (\text{A1})$$

and choose $\tilde{H}_0 = \sum_m \epsilon_m \hat{n}_m$ as the unperturbed Hamiltonian. The core Green's function can be written as³⁵

$$G_{cc}(t) = \lim_{\substack{T_1 \rightarrow -\infty \\ T_2 \rightarrow +\infty}} Q(T_2, T_1, t), \quad (\text{A2})$$

where

$$Q = -i \frac{\langle \Phi_0^N | T[\tilde{U}(T_2, T_1) \bar{a}_c(t) \bar{a}_c^\dagger] | \Phi_0^N \rangle}{\langle \Phi_0^N | \tilde{U}(T_2, T_1) | \Phi_0^N \rangle}. \quad (\text{A3})$$

$|\Phi_0^N\rangle$ is the ground state of \tilde{H}_0 , \bar{O} is an operator O in the interaction picture, and U is the time-development operator

$$\tilde{U}(T_2, T_1) = e^{i\tilde{H}_0 T_1} e^{-iH_{cv}(T_2 - T_1)} e^{-i\tilde{H}_0 T_1}. \quad (\text{A4})$$

After some straightforward algebraic manipulations all core operators can be eliminated from (A3) and we obtain for $t \leq 0$ the following result:

$$Q = ie^{-i\epsilon_c t} \frac{\langle \Phi_0^{Nv} | e^{-iH_v T_2} e^{i(H_v + V_1)t} e^{-iH_v(t - T_1)} | \Phi_0^{Nv} \rangle}{\langle \Phi_0^{Nv} | e^{iH_v(T_2 - T_1)} | \Phi_0^{Nv} \rangle}. \quad (\text{A5})$$

$|\Phi_0^{Nv}\rangle$ denotes the ground state of the unperturbed valence-electron operator $H_0 = \sum_i \epsilon_i \hat{n}_i$, $H_v = H_0 + V_v$, and V_1 is given by

$$V_1 = - \sum_{k,l} (V_{kc1c} - V_{kcc1})(a_k^\dagger a_l - n_k \delta_{kl}). \quad (\text{A6})$$

Introducing two time-development operators for the valence electrons, one (\tilde{U}_0) for the ground state and one (\tilde{U}_1) for the ionic states

$$\begin{aligned} \tilde{U}_0(T_2, T_1) &= e^{iH_0 T_2} e^{-iH_v(T_2 - T_1)} e^{-iH_0 T_1}, \\ \tilde{U}_1(T_2, T_1) &= e^{iH_0 T_2} e^{-i(H_v + V_1)(T_2 - T_1)} \\ &\quad \times e^{-iH_0 T_1}, \end{aligned} \quad (\text{A7})$$

we may write

$$Q = ie^{-i\epsilon_c t} \frac{\langle \Phi_0^{Nv} | \tilde{U}_0(T_2, 0) \tilde{U}_1(0, t) \tilde{U}_0(t, T_1) | \Phi_0^{Nv} \rangle}{\langle \Phi_0^{Nv} | \tilde{U}_0(T_2, T_1) | \Phi_0^{Nv} \rangle}. \quad (\text{A8})$$

To proceed we define an operator $\tilde{U}_t(T', T'')$ via the expansion

$$\begin{aligned} \tilde{U}_t(T', T'') &= \sum_{n=0}^{\infty} \frac{(-i)^n}{n!} \int_{T''}^{T'} dt_1 \cdots \\ &\quad \times \int_{T''}^{T'} dt_n T[\bar{V}(t_1) \cdots \bar{V}(t_n)], \end{aligned} \quad (\text{A9})$$

where

$$\bar{V}(t_i) = \bar{V}_v(t_i) + \bar{V}_1(t_i) \Theta(t_i - t) \Theta(-t_i).$$

It is clear that $\tilde{U}_0(T_2, 0) = \tilde{U}_t(T_2, 0)$, $\tilde{U}_0(t, T_1) = \tilde{U}_t(t, T_1)$, and $\tilde{U}_1(0, t) = \tilde{U}_t(0, t)$. Following Ref. (36), \tilde{U}_t defined in (A9) is a time-development operator for the time-dependent perturbation $V(t') = V_v + V_1 \Theta(t' - t) \Theta(-t')$. It follows that

$$Q = ie^{-i\epsilon_c t} R_t(T_2, T_1) / R_0(T_2, T_1), \quad (\text{A10})$$

where $R_0(T_2, T_1) = \langle \Phi_0^{Nv} | U_0(T_2, T_1) | \Phi_0^{Nv} \rangle$ and $R_t(T_2, T_1) = \langle \Phi_0^{Nv} | U_t(T_2, T_1) | \Phi_0^{Nv} \rangle$ are vacuum amplitudes³⁵ for different perturbations. The well-known linked-cluster theorem³⁵ for the vacuum amplitude states that $R(T_2, T_1) = \exp[C(T_2, T_1)]$, the function $C(T_2, T_1)$ being equal to the sum over all *connected* diagrams of $R(T_2, T_1)$:

$$\begin{aligned} C_0(T_2, T_1) &= \sum_{n=0}^{\infty} \frac{(-i)^n}{n!} \int_{T_1}^{T_2} dt_1 \cdots \int_{T_1}^{T_2} dt_n \{ \langle \Phi_0^{Nv} | T[\bar{V}_v(t_1) \cdots \bar{V}_v(t_n)] | \Phi_0^{Nv} \rangle_c \} \\ C_t(T_2, T_1) &= \sum_{n=0}^{\infty} \frac{(-i)^n}{n!} \int_{T_1}^{T_2} dt_1 \cdots \int_{T_1}^{T_2} dt_n \{ \langle \Phi_0^{Nv} | T[\bar{V}(t_1) \cdots \bar{V}(t_n)] | \Phi_0^{Nv} \rangle_c \}. \end{aligned} \quad (\text{A11})$$

With the aid of Eq. (A10) the linked-cluster theorem for the core Green's function follows immediately ($t \leq 0$)

$$G_{cc}(t) = ie^{-i\epsilon_c t} e^{C(t)}, \quad (\text{A12})$$

where

$$C(t) = \lim_{\substack{T_1 \rightarrow -\infty \\ T_2 \rightarrow +\infty}} [C_t(T_2, T_1) - C_0(T_2, T_1)].$$

$C(t)$ is equal to the sum of all connected diagrams which contain at least one interaction point. These diagrams are discussed in detail in Sec. IV B.

- ¹See, for example, J. J. Pireaux, S. Svenson, E. Basilier, P. A. Malmqvist, U. Gelius, R. Caudano, and K. Siegbahn, *Phys. Rev. A* **14**, 2133 (1976); K. Siegbahn, *J. Electron Spectrosc. Relat. Phenom.* **5**, 3 (1974); U. Gelius, *ibid.* **5**, 985 (1974); D. P. Spears, H. J. Fischbeck, and T. A. Carlson, *ibid.* **6**, 411 (1975); J. C. Fuggle, E. Umbach, D. Menzel, K. Wandelt, and C. R. Brundle, *Solid State Commun.* **27**, 65 (1978); M. Tronc, G. C. King, R. C. Bradford, and F. H. Read, *J. Phys.* **B 9**, L 555 (1976).
- ²P. S. Bagus, *Phys. Rev.* **139**, A619 (1965); P. S. Bagus and H. F. Schäfer, *J. Chem. Phys.* **55**, 1474 (1971); D. T. Clark, in *Progress in Theoretical Organic Chemistry*, Vol. 2, edited by I. G. Csizmadia (Elsevier, Amsterdam, 1977); O. Goscinski, G. Howat, and T. Åberg, *J. Phys.* **B 8**, 11 (1975); D. Firsh, B. T. Pickup, and R. McWeeny, *Chem. Phys.* **29**, 67 (1978).
- ³M. F. Guest, I. H. Hillier, V. R. Saunders, and M. H. Wood, *Proc. R. Soc. London A* **333**, 201 (1973); H. Basch, *Chem. Phys. Lett.* **37**, 443 (1976); K. Radler, B. Sonntag, T. C. Chang, and W. H. E. Schwarz, *Chem. Phys.* **13**, 363 (1976); W. Butscher, R. J. Buenker, and S. D. Peyerimhoff, *Chem. Phys. Lett.* **52**, 449 (1977); R. L. Martin and D. A. Shirley, *J. Chem. Phys.* **64**, 3684 (1976); W. A. Goddard III and W. J. Hunt, *Chem. Phys. Lett.* **24**, 464 (1974).
- ⁴See, for example. (a) G. D. Mahan, *Solid State Phys.* **29**, 75 (1974); (b) D. C. Langreth, *Phys. Rev. B* **1**, 471 (1970); (c) S. Doniach and M. Sunjic, *J. Phys. C* **3**, 285 (1970); (d) V. I. Grebennikov, O. B. Sokolov, and E. A. Turov, *Phys. Status Solidi B* **84**, 773 (1977).
- ⁵See, for example, K. Schönhammer and O. Gunnarsson, *Phys. Rev. B* **18**, 6606 (1978).
- ⁶W. Domcke, L. S. Cederbaum, J. Schirmer, and W. von Niessen, *Phys. Rev. Lett.* **42**, 1237 (1979).
- ⁷P. O. Löwdin, *Adv. Chem. Phys.* **14**, 283 (1969).
- ⁸C. C. J. Roothaan, *Rev. Mod. Phys.* **23**, 69 (1951); **32**, 179 (1960).
- ⁹When the core shell is not closed, the solutions ψ_i of the Schrödinger equation are not necessarily given as a simple (antisymmetrized) product $\Psi(\text{core})\Psi(\text{valence})$. In order to meet the requirement that the ψ_i are eigenfunctions of the spin operators \hat{S}^2 and \hat{S}_z , the Ψ_i may be a superposition of a few products.
- ¹⁰It should be emphasized that the conclusions are drawn in the context of the ground state HF; i.e., the interaction between core and valence electrons is already taken into account on the HF level.
- ¹¹U. Gelius, S. Svensson, H. Siegbahn, E. Basilier, A. Faxälv, and K. Siegbahn, *Chem. Phys. Lett.* **28**, 1 (1974).
- ¹²P. H. Citrin, P. Eisenberger, and D. R. Hamann, *Phys. Rev. Lett.* **33**, 965 (1974).
- ¹³W. Domcke and L. S. Cederbaum, *Chem. Phys. Lett.* **31**, 582 (1975).
- ¹⁴A. Denis, J. Langlet, and J. P. Malrieu, *Theor. Chim. Acta* **38**, 49 (1975); L. S. Cederbaum and W. Domcke, *J. Chem. Phys.* **66**, 5085 (1977).
- ¹⁵P. S. Bagus and J. F. Schaefer, *J. Chem. Phys.* **56**, 224 (1972).
- ¹⁶A. B. Migdal, *J. Phys. (Moscow)* **4**, 449 (1941); E. L. Feinberg, *ibid.* **4**, 424 (1941).
- ¹⁷T. Åberg, *Phys. Rev.* **156**, 35 (1967).
- ¹⁸L. S. Cederbaum and W. Domcke, *Adv. Chem. Phys.* **36**, 205 (1977).
- ¹⁹D. J. Thouless, *The Quantum Mechanics of Many-Body Systems* (Academic, New York, 1961).
- ²⁰A. Abrikosov, L. Gorkov, and J. Dzyaloshinski, *Quantum Field Methods in Statistical Physics*, 2nd ed., edited by D. ter Haan (Pergamon, New York, 1965).
- ²¹L. S. Cederbaum, W. Domcke, H. Köppel, and W. von Niessen, *Chem. Phys.* **26**, 149 (1977).
- ²²B. T. Pickup and O. Goscinski, *Mol. Phys.* **26**, 1013 (1973).
- ²³G. Born, H. A. Kurtz, and Y. Öhrn, *J. Chem. Phys.* **68**, 74 (1978).
- ²⁴P. Nozieres and C. T. DeDominicis, *Phys. Rev.* **178**, 1097 (1969).
- ²⁵A. B. Migdal, *Theory of Finite Fermi Systems and Applications to Atomic Nuclei* (Interscience, New York, 1967).
- ²⁶G. D. Purvis and Y. Öhrn, *J. Chem. Phys.* **60**, 4063 (1974); P. O. Nerbrant, *Int. J. Quantum Chem.* **9**, 901 (1975).
- ²⁷J. Schirmer and L. S. Cederbaum, *J. Phys.* **B 11**, 1889 (1978).
- ²⁸K. Siegbahn, *J. Electron. Spectrosc. Relat. Phenom.* **5**, 3 (1974).
- ²⁹L. J. Arons, M. Barber, M. F. Guest, I. H. Hillier, and J. H. McCartney, *Mol. Phys.* **26**, 1247 (1973).
- ³⁰M. H. Wood, *Chem. Phys.* **5**, 471 (1974).
- ³¹S. Svenson, H. Ågren, and U. I. Wahlgren, *Chem. Phys. Lett.* **38**, 1 (1976).
- ³²U. Wahlgren, *Mol. Phys.* **33**, 1109 (1977).
- ³³W. von Niessen (unpublished).
- ³⁴G. H. F. Diercksen and W. P. Kraemer, MUNICH, Molecular Program System, Reference Manual, Special Technical Report, Max-Planck Institut für Physik und Astrophysik (in press); G. H. F. Diercksen, *Theor. Chim. Acta* **33**, 1 (1974).
- ³⁵R. D. Mattuck, *A Guide to Feynman Diagrams in the Many-Body Problem* (McGraw-Hill, New York, 1967), p. 255 ff.
- ³⁶A. L. Fetter and J. D. Walecka, *Quantum Theory of Many-Particle Systems* (McGraw-Hill, New York, 1971), p. 60.
- ³⁷R. Manne and T. Åberg, *Chem. Phys. Lett.* **7**, 282 (1970).